

Article

Photoinduced Electron Transfer and Aggregation-Induced Emission in 1,8-Naphthalimide Probes as a Platform for Detection of Acid/Base Vapors

Nikolai I. Georgiev ^{1,*} , Ventsislav V. Bakov ¹  and Vladimir B. Bojinov ^{1,2,*} 

¹ Department of Organic Synthesis, University of Chemical Technology and Metallurgy, 8 Kliment Ohridsky Str., 1756 Sofia, Bulgaria

² Bulgarian Academy of Sciences, 1040 Sofia, Bulgaria

* Correspondence: nikigeorgiev@uctm.edu (N.I.G.); vlbojin@uctm.edu (V.B.B.); Tel.: +359-2-8163207 (N.I.G.); +359-2-8163206 (V.B.B.)

Abstract: In the last few decades, photoinduced electron transfer (PET) based on “fluorophore-spacer-receptor” format became the most popular approach in the design of fluorescent sensing probes. As a result, a variety of architectures for detection of different chemical species has been synthesized, and PET has been well-studied in liquid solutions. The extension of the principles of molecular sensors from liquid solution onto solid support is currently a major task, which opens up new directions for practical applications. An approach for the design of solid state fluorescence-sensing materials could be based on aggregation-induced emission (AIE). That is why, herein, we focused our attention on the investigation of some 1,8-naphthalimides designed on classical “fluorophore-spacer-receptor” to serve as fluorescence-sensing materials in solid state via simultaneous PET and AIE. The effects of different substituents were investigated, and it was found that the examined compounds with well-pronounced AIE could be used as an efficient platform for rapid detection of pH and acid/base vapors in solid state.

Keywords: 1,8-naphthalimide; fluorescent sensors; photoinduced electron transfer (PET); solid state emission; acid-base vapors; strip paper; aggregation-induced emission (AIE)



Citation: Georgiev, N.I.; Bakov, V.V.; Bojinov, V.B. Photoinduced Electron Transfer and Aggregation-Induced Emission in 1,8-Naphthalimide Probes as a Platform for Detection of Acid/Base Vapors. *Photonics* **2022**, *9*, 994. <https://doi.org/10.3390/photonics9120994>

Received: 25 November 2022

Accepted: 15 December 2022

Published: 16 December 2022

Publisher's Note: MDPI stays neutral with regard to jurisdictional claims in published maps and institutional affiliations.



Copyright: © 2022 by the authors. Licensee MDPI, Basel, Switzerland. This article is an open access article distributed under the terms and conditions of the Creative Commons Attribution (CC BY) license (<https://creativecommons.org/licenses/by/4.0/>).

1. Introduction

Owing to their importance in health care and environmental protection, great attention is currently being paid to the design and synthesis of novel fluorescence probes [1–4]. Generally, their attractiveness was based on the utilized fluorescent signaling output and its benefits such as immediate response, high efficiency and sensitivity, cheap and affordable equipment suitable even for field analysis [5,6]. In addition, the used fluorescence techniques for analysis allow noninvasive and harmless real-time imaging with great spectral resolution in living objects that is extremely useful for modern biomedical applications [6–12].

The intensive work in this field resulted in a large number of fluorescent probes for detection of different chemical species, which were based on a few photophysical phenomena, including intramolecular charge transfer (ICT), twisted intramolecular charge transfer (TICT), photoinduced electron transfer (PET), fluorescence resonance energy transfer (FRET), excited-state intramolecular proton transfer (ESIPT) and aggregation-induced emission (AIE) [13–27]. Among them, the PET model developed by A. P. de Silva using “fluorophore-spacer-receptor” became the most popular approach for the design of fluorescence-sensing probes [28–32]. Notably, this model was distinguishable with having simple construction and easy and predictable communication between the receptor (recognition part) and the fluorophore (signaling part). That is why, in the last few decades, the PET process was well-studied in the most common fluorophores, and a large variety of

PET probes was reported. Furthermore, the PET probes based on the “fluorophore-spacer-receptor” format were successfully implemented even in molecular logic gates for a more complex analysis [33–37]. However, the design and synthesis of novel PET fluorescent probes with improved properties and better applicability is still a great challenge. Thus, extension of the principles of molecular sensors from liquid solution onto solid support is currently a major task that opens up new directions for practical applications [38–40].

An approach for the design of solid state fluorescence-sensing materials could be based on aggregation-induced emission (AIE). AIE is a relatively new strategy for the design of fluorescence probes that is currently very attractive due to the observed unusual high emission output in solid state and the lack of fluorescence in solution [41,42]. This phenomenon showed the opposite results in comparison with the traditional organic fluorophores that possessed bright fluorescence only in dilute solutions. The different behavior of AIE probes inspired the research interest of the development of a new concept for the design of fluorescent materials, particularly with practical applications in the fields of OLED and chemosensing systems [43–45]. However, the reports about simultaneous acting PET processes and AIE in organic fluorophores are very rare.

Recently, we prepared a fluorescence-sensing 1,8-naphthalimide-based probe in the classical PET “fluorophore-spacer-receptor” format, which showed latent fluorescence in an aggregated state due to the PET quenching process [46]. This compound was successfully applied as a solid state chemosensing material for rapid detection of acid/base vapors and pH in aqueous solutions due to the reversible modulation of PET after exposure to acid/base vapors. These results encouraged us to extend this concept to variety of 1,8-naphthalimide derivatives and to determine the influence of different substituents on the effectiveness of the probes.

2. Materials and Methods

2.1. Materials

Commercially available 1,8-naftalic anhydride, 4-chloro-1,8-naftalic anhydride, 4-bromo-1,8-naftalic anhydride, 4-nitro-1,8-naphthalic anhydride, *n*-butylamine, ethylenediamine, *N,N*-dimethylethylenediamine, *N*-(2-hydroxyethyl)ethylenediamine, *N*-methylpiperazine, allyl amine, allyl alcohol, chloroacetyl chloride and methyl acrylate (Sigma-Aldrich Co., St. Louis, MO, USA and Fisher Scientific, Waltham, MA, USA) were used as purchased without further purification. 1,8-Naphthalimides 1–4 and 7–11 were synthesized as described before [47–51]. The intermediate compound *N*-[2-(2-hydroxyethylamino)-ethyl]-1,8-naphthalimide 5 was synthesized according to the previously reported procedure [52]. The solvents used in the synthetic procedures and in the photophysical investigation, HCl and NH₃ (Sigma-Aldrich Co., Ltd., St. Louis, MO, USA and Fisher Scientific, Waltham, MA, USA), were pure or of spectroscopy grade.

2.2. Methods

FT-IR spectra were recorded on a Thermo Scientific Nicolet iS20 FTIR spectrometer (Thermo Fisher Scientific, Waltham, MA, USA). The ¹H NMR analysis was performed on a Bruker AV-600 spectrometer (BRUKER AVANCE II+ 600 MHz, Bruker, Billerica, MA, USA) with an operating frequency at 600 MHz. Electrospray ionization mass spectra (ESI-MS) were obtained on a Bruker MicrOTOF-Q system (Compass, Bruker, Billerica, MA, USA). The elemental analysis data were obtained on an automated EuroEA3000 CHNS-O Analyzer (Euro Vector S.P.A, Pavia PV, Italy). The TLC monitoring was performed on silica gel, ALUGRAM[®]SIL G/UV254, 40 × 80 mm, 0.2 mm silica gel 60. A Hewlett-Packard 8452A spectrophotometer (Agilent Technologies, Inc., Santa Clara, CA, USA) was used for the UV-Vis absorption measurements. The photophysical study was performed at room temperature (25.0 °C) in 1 × 1 cm quartz cuvettes. The fluorescence spectra were recorded using a Scinco FS-2 spectrofluorimeter (Scinco, Seoul, Korea). The solid films were obtained by deposition of the probe solutions on a glass plate and evaporation of the solvent.

2.3. Synthetic Procedures

Synthesis of 1,8-Naphthalimide 6

To a solution of methyl acrylate (6.3 mL, 20 mmol) in 10 mL of methanol, a solution of 1,8-naphthalimide 5 (1 g, 3.5 mmol) in 10 mL of methanol was added dropwise for a period of 30 min. The reaction mixture was stirred for 3 days at room temperature, and the excess of methyl acrylate was removed under vacuum, whereupon the ester-functionalized derivative 6 was obtained as yellow-brown oil (1.27 g, 98%). FT-IR (KBr) cm^{-1} : 1732 (ν MeO-C=O); 1701 (ν^{as} N-C=O); 1648 (ν^{s} N-C=O). $^1\text{H NMR}$ (CHCl_3-d , 600.13 MHz) δ 8.63 (dd, 2H, $J = 7.3$ Hz, $J = 1.1$ Hz, naphthalimide H-2 and H-7), 8.25 (dd, 2H, $J = 8.2$ Hz, $J = 1.1$ Hz, naphthalimide H-4 and H-5), 7.78 (dd, 2H, $J = 8.2$ Hz, $J = 7.3$ Hz, naphthalimide H-3 and H-6), 4.31 (t, 2H, $J = 6.7$ Hz, $(\text{CO})_2\text{NCH}_2$), 3.65 (dd, 2H, $J = 6.4$ Hz, $J = 3.7$ Hz, $\text{CH}_2\text{CH}_2\text{CO}$), 3.49 (s, 3H, OCH_3), 2.90 (m, 4H, $\text{NCH}_2\text{CH}_2\text{OH}$), 2.80 (dd, 2H, $J = 6.4$ Hz, $J = 3.7$ Hz, $\text{CH}_2\text{CH}_2\text{CO}$) and 2.46 (t, 2H, $J = 6.7$ Hz, $(\text{CO})_2\text{NCH}_2\text{CH}_2$). Calculated for $\text{C}_{20}\text{H}_{22}\text{N}_2\text{O}_5$ (MW 370.40) C 64.85, H 5.99, N 7.56%; found C 65.02, H 6.05, N 7.47%. Positive-ion ESI-MS at m/z : 371.0122 $[\text{M} + \text{H}]^+$.

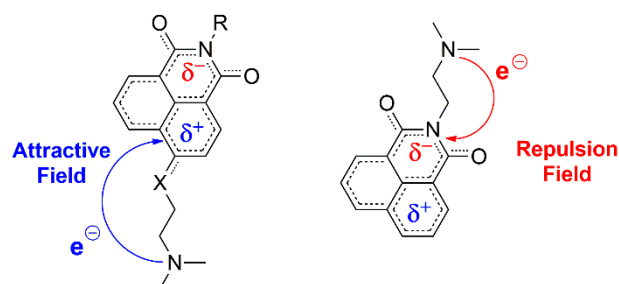
3. Results and Discussion

3.1. Design and Synthesis

We focused our study on the 1,8-naphthalimide fluorogenic molecules due to their bright fluorescence, large Stokes shifts and high photo and chemical stability [53,54]. All compounds under study were designed as PET fluorescent probes based on a classical “fluorophore-spacer-receptor” model where the electron-rich tertiary amine is the proton receptor and the 1,8-naphthalimide fluorophore is the fluorescence signaling part. The rational synthetic methods for obtaining 1,8-naphthalimide chemosensors allows two possibilities for incorporation of PET receptor fragments in this fluorophoric system. For the first one, the receptor fragment known as “Upper-receptor” is bound to *N*-position of the 1,8-naphthalimide architecture, while in the second one, the receptor fragment named “Lower-receptor” is directly attached to a C-4 position of the 1,8-naphthalimide fluorophore [55].

Thermodynamically, both PET paths from the unprotonated amino receptors are feasibly equal but require the electron to enter the fluorophore across a different electric field, which affects its efficiency [47,56]. It is well-known that the 1,8-naphthalimide fluorophoric system is an ICT “push-pull” π -electron system where, in the excited state, strong charge transfer occurs from the C-4 electron-donating position to the carbonyl electron-accepting groups, and considerable dipole character is generated (negative pole at the imide terminus) [57,58]. A large dipole moment in the excited state gives rise to a strong photogenerated electric field. Depending on its charge and magnitude, this molecular electric field could inhibit or accelerate a transiting electron in the 1,8-naphthalimide excited state. Thus, the fluorescence-quenching PET process is accelerated in the “Lower-receptors” systems, where the electrons enter the space of the 1,8-naphthalimide fluorophore across its attractive electric field (Scheme 1).

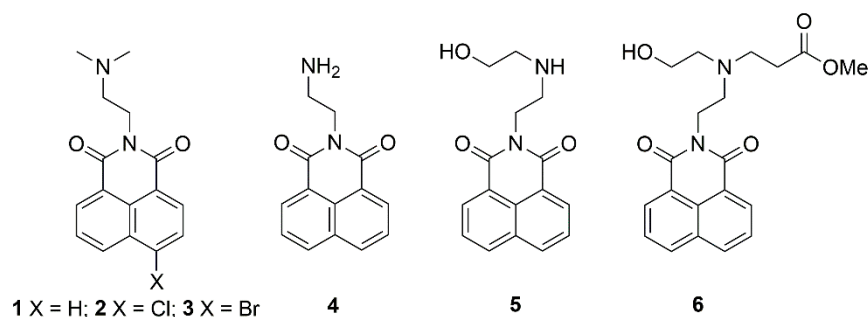
LOWER RECEPTOR SYSTEM UPPER RECEPTOR SYSTEM



Scheme 1. Dipole character and PET direction in 1,8-naphthalimide “lower” and “upper” receptor systems.

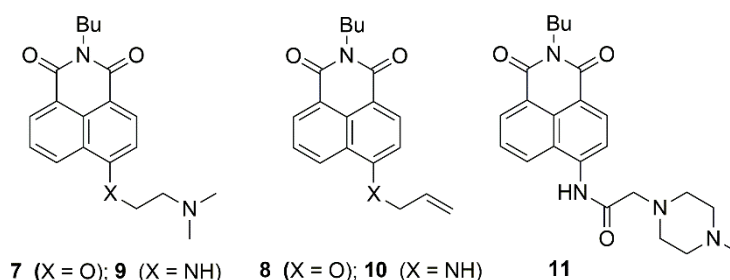
However, in the “Upper-receptor” systems, the strong repulsive character of the resulted field around the imide moiety seriously restricts the PET process from the *N*-position in the electron-rich architectures such as 4-amino-1,8-naphthalimides [59–61].

This effect is reduced in the unsubstituted or 4-halogen-substituted electron-poorer derivatives, which generate a weaker repulsive field around the imide cycle of the fluorophore [48,62]. That is why we chose the C-4 unsubstituted and 4-c-halogeno-substituted 1,8-naphthalimide units during the study of “Upper-receptor” systems instead of the commonly used 4-amino- or 4-oxy-substituted derivatives (Scheme 2).



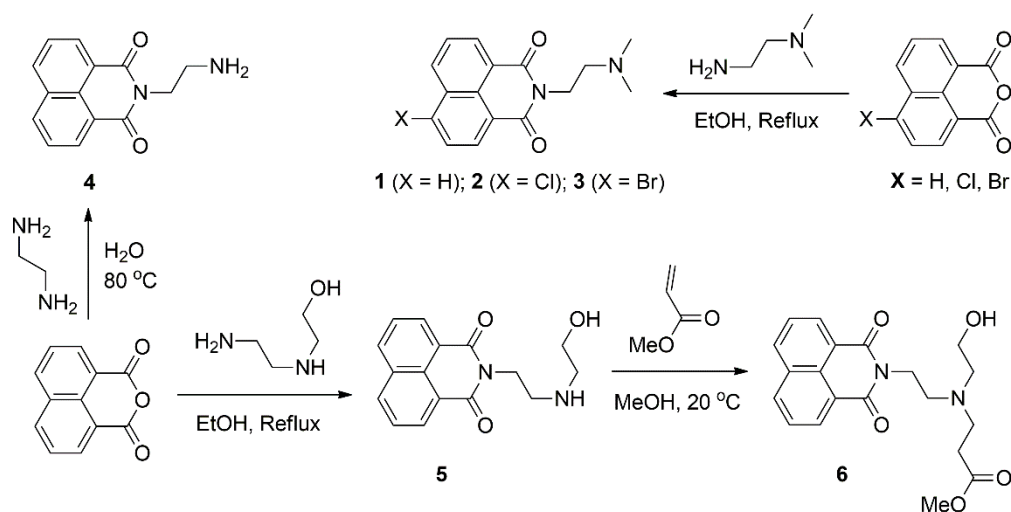
Scheme 2. Chemical structure of 1,8-naphthalimide-based “Upper-receptor” systems 1–6.

Furthermore, the effect of the “Lower-receptors” was investigated in common 4-oxy, 4-amino and 4-amido 1,8-naphthalimides (Scheme 3).



Scheme 3. Chemical structure of 1,8-naphthalimide-based “Lower-receptor” systems 7–11.

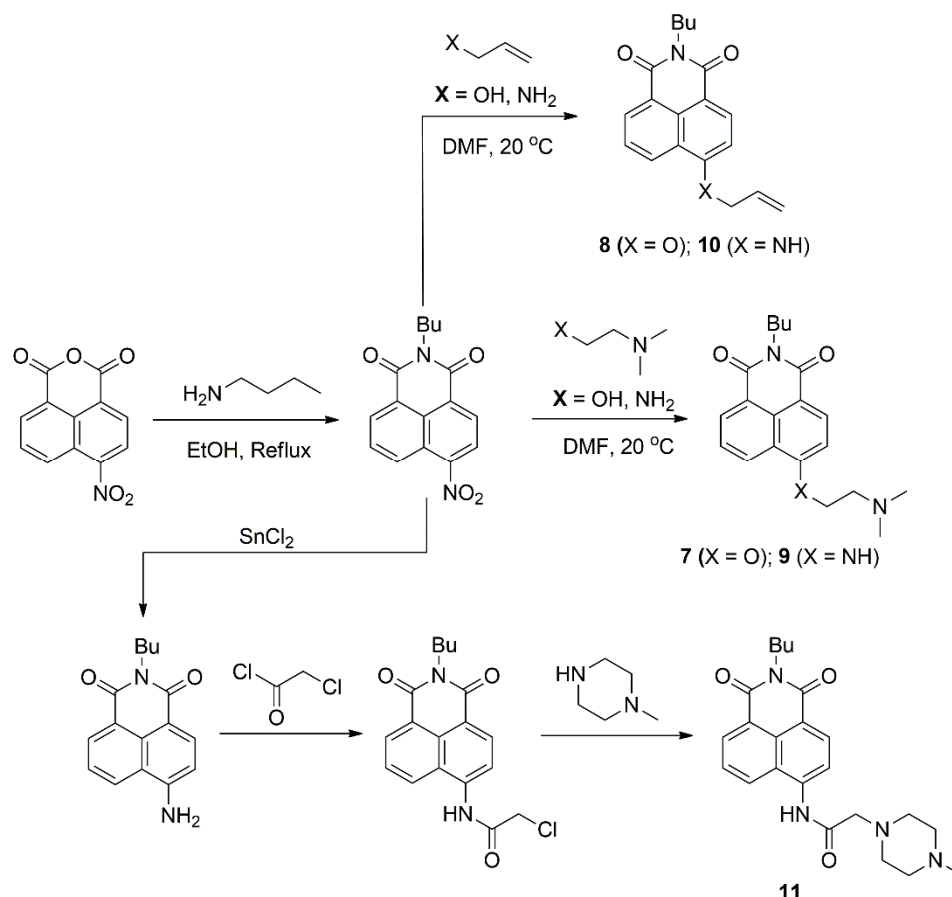
The 1,8-naphthalimides containing PET “Upper receptor” fragments were synthesized according to Scheme 4 using available sources.



Scheme 4. Synthesis of 1,8-naphthalimides 1–6.

Compounds 1–3 and 5 were obtained according to previous reports [49,50,52] after condensation of 1,8-naphthalic anhydride or 4-halogeno-1,8-naphthalic anhydride with the corresponding amines (*N,N*-dimethylethylenediamine or *N*-(2-hydroxyethyl)ethylenediamine) in boiling ethanol. 1,8-Naphthalimide 4 was prepared, as we reported before, by interaction of ethylene diamine and 1,8-naphthalic anhydride in water [47]. The novel PET probe 6 was synthesized after Michael addition of methyl acrylate to 1,8-naphthalimide 5 at room temperature in methanol.

The 1,8-naphthalimides under study containing “Lower receptors” were synthesized, as we reported before, according to Scheme 5 [40,63].



Scheme 5. Synthesis of 1,8-naphthalimides 7–11.

All compounds were obtained from intermediate 4-nitro-1,8-naphthalimide that was synthesized after reaction of *n*-butylamine with 4-nitro-naphthalic anhydride in boiling ethanol. The reference compounds 8 and 10 were prepared after nucleophilic substitution of the nitro group with allyl amine or allyl alcohol in DMF at room temperature. The PET probes 7 and 9 were obtained similarly to 8 and 10 using *N,N*-dimethylethylenediamine or *N*-dimethylethanolamine instead of allyl amine and allyl alcohol. The 1,8-naphthalimide 11 was prepared in three steps, as we reported before [63]. In first step, the *N*-butyl-4-nitro-1,8-naphthalimide was reduced selectively to *N*-butyl-4-amino-1,8-naphthalimide using SnCl_2 . Then, the amino group was acetylated with chloroacetyl chloride, and the obtained intermediate was reacted with methylpiperazine to afford the fluorescence probe 11.

The 1,8-naphthalimides under study were prepared as solid state emissive probes with PET fluorescence-sensing signaling output. In order to examine the PET process in solid state, all of the compounds were dissolved in a 1:1 binary solvent mixture of ethanol and chloroform. Then, the so-prepared saturated solutions (10^{-2} M) were sprayed onto a glass, and the solvent was evaporated in air. The resulted film was exposed for 2 s to HCl

and then to NH_3 vapors. The glass samples were photographed, and their fluorescence spectra were recorded after each exposure.

3.2. Chemosensing Properties

3.2.1. 1,8-Naphthalimides Containing “Upper-Receptor”

The 1,8-naphthalimide **1** is a typical fluorescence-sensing system based on the “fluorophore-spacer-receptor” format with well-pronounced PET [50]. Due to the PET process, compound **1** showed a very low fluorescence emission in diluted solution. After protonation of the tertiary amino receptor, the PET quenching process was cut off, and bright fluorescence appeared in a range of 350–500 nm with a maximum at 396 nm (Figure 1).

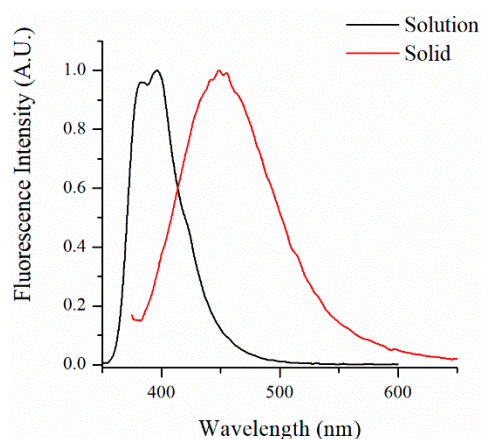


Figure 1. Normalized fluorescence spectra of probe **1** in water solution at pH 4 and thin film of probe **1** exposed to HCl vapors.

In concentrated solution, compound **1** displayed low green fluorescence that decreased after dilution (Figure 2a). The observed green fluorescence in concentrated solutions was usual for unsubstituted and 4-halogeno-substituted 1,8-naphthalimides, as it was attributed to aggregation-induced emission (AIE). However, the previously reported 1,8-naphthalimides showed a much stronger fluorescence, probably due to the lack of a PET quenching process in their architectures. To confirm this statement, a powder of **1** was exposed to acid vapors (HCl) and, under a UV-lamp ($\lambda = 366$ nm), was found that due to the prevented PET, compound **1** has a bright emission in aggregated state after exposure of acid vapors (Figure 2b). Obviously, the observed fluorescence properties of **1** were based on the simultaneous acting latent AIE and quenching PET. The use of powder for sensing purposes is inappropriate, which is why probe **1** was studied in thin film on glass support as a fluorescence-sensing material in aggregated state. However, in order to obtain latent AIE, the thin films were prepared from concentrated solutions containing 10^{-2} M of compound **1**; otherwise, the use of diluted solutions resulted in a dominant monomeric fluorescence emission.

Similarly to the diluted solution, the prepared thin film based on probe **1** showed low fluorescence before exposure to HCl vapors and highly intensive fluorescence emission due to the disallowed PET after exposure (Figure 3), which was visible even to a naked eye (Figure 4). However, the observed fluorescence was broad and in the spectral region of between 370 nm and 600 nm, with a maximum at 450 nm (Figure 1). The observed red-shifting fluorescence spectrum of probe **1** in an aggregated state compared to that in diluted solution was expectable, and it could be explained with the formation of J-aggregates [64,65]. According to Kasha’s exciton theory in J-aggregation, the state of the molecule is regarded as a dipole, and the excitonic state of the aggregate splits into two levels through the interaction of transition dipoles.

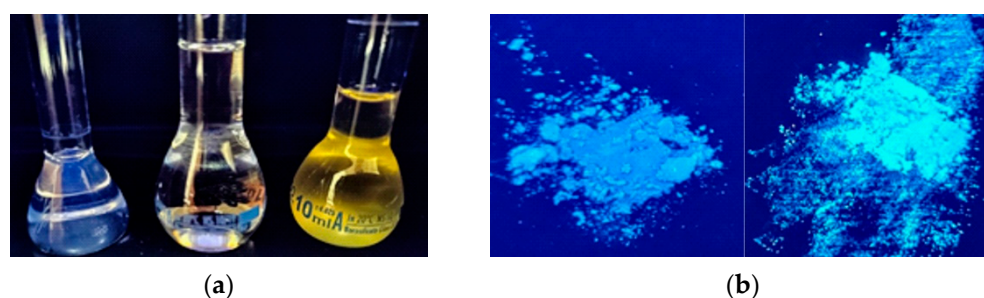


Figure 2. (a) Solutions of **1** in DMSO at 10^{-4} M (left), 10^{-3} M (middle) and 10^{-2} M (right) and (b) powder of probe **1** before (left) and after (right) exposure to HCl vapors.

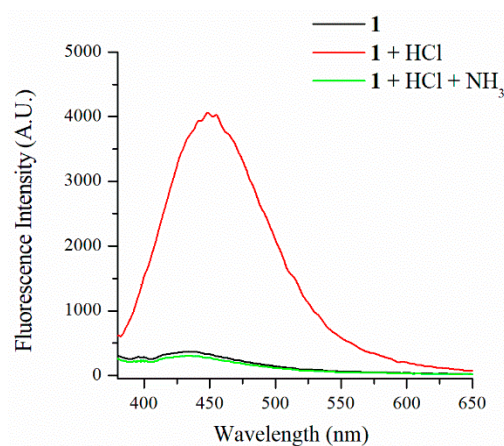


Figure 3. Fluorescence spectra of solid film of probe **1**, exposed first to HCl and then to NH_3 vapors ($\lambda_{\text{ex}} = 370$ nm).

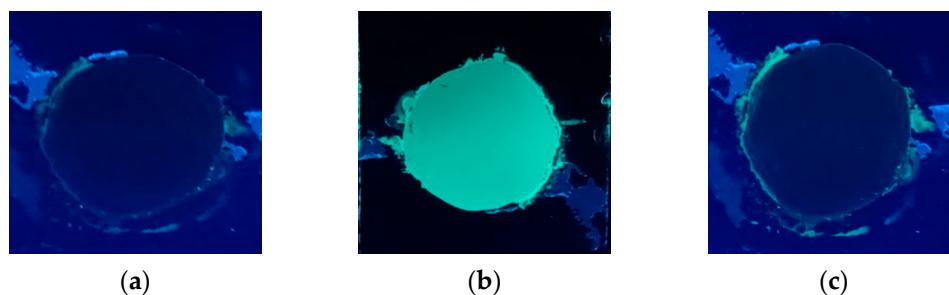


Figure 4. Solid film of probe **1** under UV lamp (a) exposed first to HCl (b) and then to NH_3 (c) vapors.

It was found that the bright fluorescence of the thin film of compound **1** exposed to HCl vapors could be turned “off” to its initial state after exposure to NH_3 vapors (Figure 3). In addition, the emission of the thin film was transferred between “off” and “on” state reversibly 10 times without significant changes in both states. The observed fluorescence enhancement was calculated to be $\text{FE} = 13.3$ (the maximum fluorescence intensity of the compound when exposed to hydrochloric vapors divided by the maximum fluorescence intensity after exposure to ammonia vapors). Furthermore, the resulting fluorescent and nonfluorescent films showed stable fluorescent output at room conditions for at least 2 weeks. These results clearly showed that compound **1** could be used as an efficient platform for the rapid detection of acid/base vapors in solid state.

Paper is a promising material for fabrication of smart devices such as chemosensors because it allows easier operation and portability at very low cost [66–69]. That is why a solution of **1** was poured onto a filter paper and the solvent was evaporated in order to obtain strip papers with chemosensing properties. The so-prepared strip papers showed exactly

the same fluorescent response toward acid/base vapors as the filmed glass plate. Additionally, their ability to determine pH in aqueous solution was studied and found that the obtained strip papers based on compound **1** are a suitable indicator for the determination of pHs in a pH window 2.5–1.5 (Figure 5).

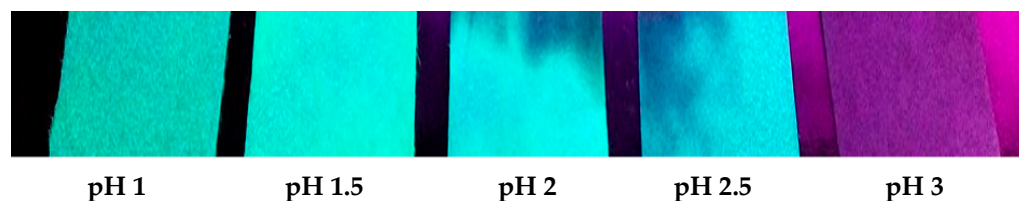


Figure 5. Fluorescent response of strip papers based on 1,8-naphthalimide **1** at different pHs.

In order to determine the solid state chemosensing properties and the influence of the C-4 substituents of 4-halogen-substituted 1,8-naphthalimides based on the classic PET “fluorophore-spacer-receptor” format, compounds **2** and **3**, containing chlorine and bromine in the C-4 position, were also involved in the present study. It was found that the C-4 halogen favored the solid state emission in the 1,8-naphthalimide PET system and the effect of the different C-4 halogens was negligible (Figure 6). As can be seen from Figure 6A, after exposure to HCl, the thin film of compounds **2** and **3** showed bright fluorescence in the range of 400–600 nm, with a maximum at about 480 nm. Similarly to compound **1**, both films reversibly turned their emission between the “off” and “on” state after exposure to HCl and NH₃ vapors (Figure 6B) several times, as the observed fluorescence enhancement was more than 60 times (FE = 64.2). The prepared strip papers from compounds **2** and **3** showed exactly the same response as probe **1**.

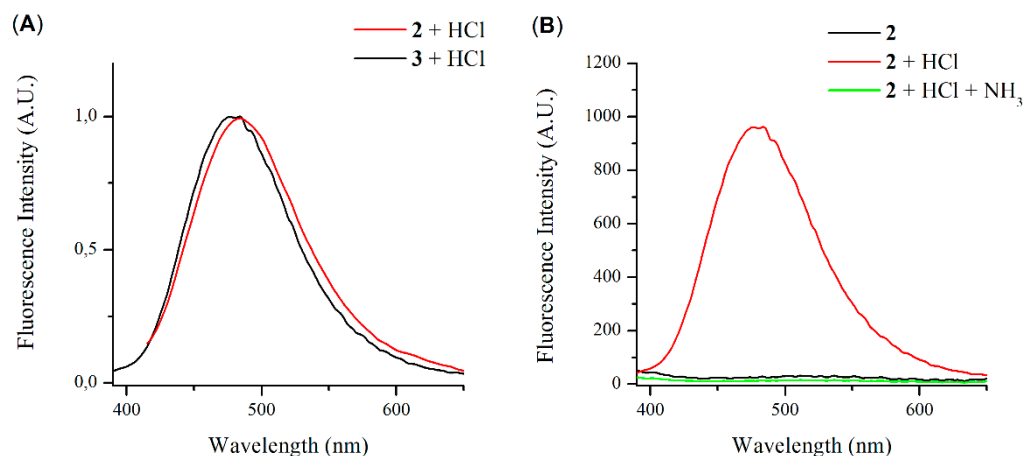


Figure 6. Normalized fluorescence spectra of thin films of **2** and **3** ($\lambda_{\text{ex}} = 370$ nm) exposed to HCl vapors (A) and fluorescence spectra of solid film of probe **2**, exposed first to HCl and then to NH₃ vapors (B).

Furthermore, the thin film of compound **4** was studied after exposure to HCl and NH₃ in order to determine the ability of primary amine to serve as a PET proton receptor in aggregated state. The results obtained were consistent with those in solution. The thin film of **4** showed well-pronounced AIE centered at 513 nm due to the possibility of primary amine to participate in hydrogen bonding, which stimulates AIE. However, the observed films showed a weak chemosensing response due to the lower oxidation potential of the primary amine, which lowered the feasibility of the PET process. The observed fluorescence enhancement after exposure to HCl and NH₃ vapors was FE = 1.4 (Figure 7).

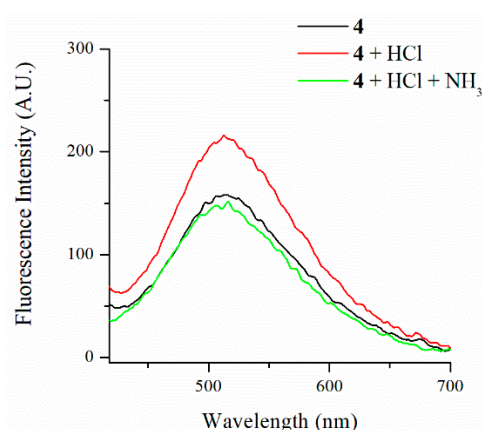


Figure 7. Fluorescence spectra of solid film of probe **4**, exposed first to HCl and then to NH_3 vapors ($\lambda_{\text{ex}} = 370 \text{ nm}$).

The above results showed the great potential of the PET-based 1,8-naphthalimides with “Upper-receptor” to serve as efficient probes for rapid detection of acid/base vapors in solid state. However, the introduction of amines in 1,8-naphthalimides’ *N*-position increased their water solubility and could affect the thin film stability in the presence of water vapors. That is why, herein, the chemosensing properties of thin film based on compound **5**, which was well-known as a highly water-soluble PET probe [52], was studied and why the observed results were compared with a similar compound, **6**, with higher hydrophobicity. Both compounds have a very similar fluorescence-sensing behavior in aggregated state. After exposure to HCl, the thin films based on **5** and **6** showed, due to the hindered PET, a bright fluorescence, with a maximum at 490 nm (Figure 8). Additionally, both films were switched reversible between the “off” and “on” states using HCl and NH_3 vapors with fluorescence enhancement about 60 times (FE = 56.2 for compound **5** and FE = 59.5 for compound **6**).

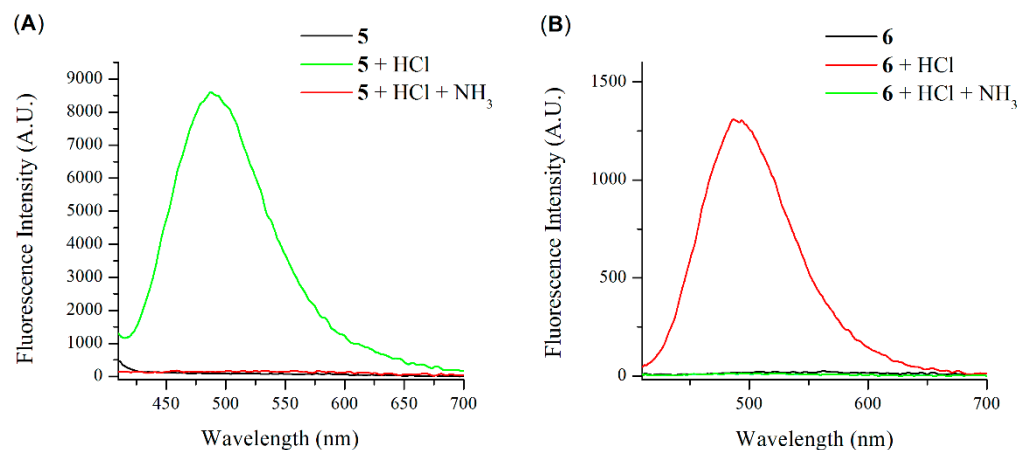


Figure 8. Fluorescence spectra of solid film of probe **5** (A) and probe **6** (B), exposed first to HCl and then to NH_3 vapors ($\lambda_{\text{ex}} = 370 \text{ nm}$).

However, due to the different solubility, both films showed different stability after exposure to water vapors. As can be seen from Figure 9, the thin film based on compound **5** showed a monomeric blue emission due to the dissolved molecules on the surface (Figure 9a). At the same time, the thin film based on compound **6** showed a constant starting green emission (Figure 9b).

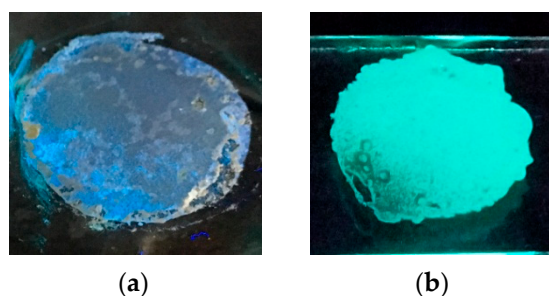


Figure 9. Solid film under UV lamp of probe 5 (a) and probe 6 (b), exposed to water vapors.

3.2.2. 1,8-Naphthalimides Containing “Lower-Receptor”

Due to their strong emission in the visible spectral region, the most common PET sensing 1,8-naphthalimides are their 4-amino, 4-oxy and 4-amido substituted derivatives. However, they possess a strong electron-donating group in the C-4 position of the fluorophoric system, which generates a strong electron repulsive field around the imide group in the excited state, and the PET in these systems usually occurs only in architectures with a “Lower-receptor” fragment.

Compound 7 is a typical 4-oxy-substituted PET probe containing “Lower-receptor”. In thin film, it showed low fluorescence emission, which was amplified after exposure to HCl vapors about 10 times due the protonation of the tertiary amino receptor, which prevented PET quenching process. The fluorescence spectrum of 7 in thin film was completely different in comparison with the above registered for the “Upper-receptor” PET systems in the “on” state. As can be seen from Figure 10, the solid state fluorescence emission of 7 showed two well-pronounced bands centered at 452 nm and 562 nm. These bands could be attributed to the presence of both monomeric and aggregation-induced emission in solid state [44]. In order to conform this assumption, 1,8-naphthalimide 8 without PET receptor was also investigated as thin film on glass support. As we expected, the fluorescence spectrum of compound 8 in solid state was similar compared to the fluorescence spectrum of 7, but with monomeric emission at 436 nm, aggregation-induced emission at 492 nm and lack of chemosensing response.

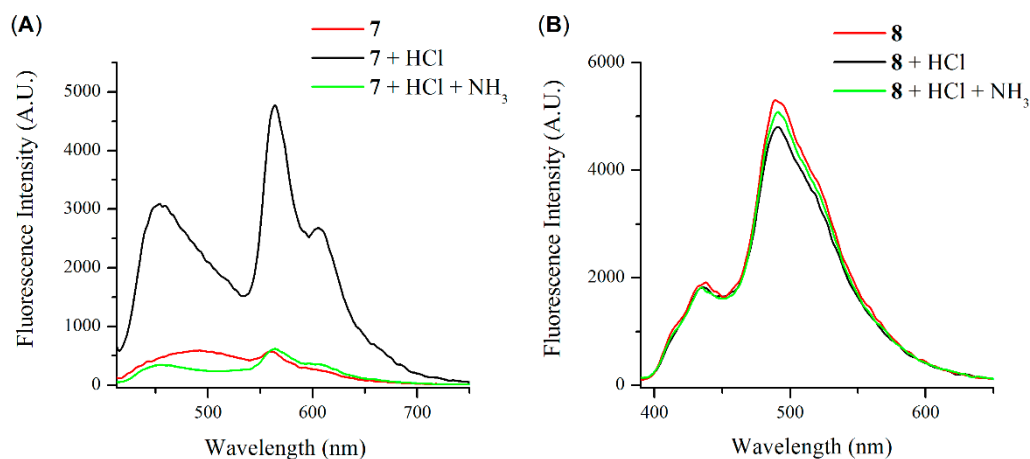


Figure 10. Fluorescence spectra of solid film of probe 7 (A) and compound 8 (B), exposed first to HCl and then to NH₃ vapors ($\lambda_{\text{ex}} = 370$ nm).

The thin film based on 7 showed a reversible fluorescence response after exposure to HCl and NH₃ vapors (Figure 11), as the observed “off” and “on” states showed constant and stable fluorescence output for at least two weeks.

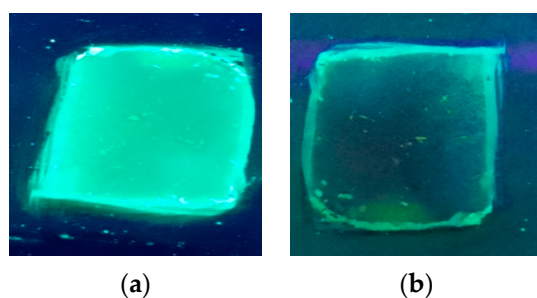


Figure 11. Solid film of probe 7 under UV lamp exposed first to HCl (a) and then to NH_3 (b) vapors.

In addition, the prepared strip papers from compound 7 showed pH fluorescence-sensing properties exactly in the same pH window as the above studied compounds possessing “Upper-receptor” (Figure 12). This result clearly illustrates that the different substituents do not show any effect on the PET sensing response in 1,8-naphthalimides on the strip paper.

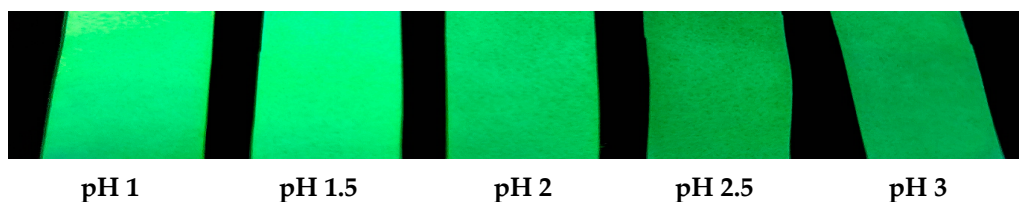


Figure 12. Fluorescent response of strip papers based on 1,8-naphthalimide 7 at different pHs.

For a difference of compound 7, the 4-amino substituted PET probe 9 in thin film showed a very low fluorescence emission centered at 550 nm with negligible sensing properties toward HCl and NH_3 vapors (Figure 13A). The resulted fluorescence placed around the monomeric emission of 4-amino-1,8-naphthalimide in solid film of 9 could be attributed to the lack of aggregation-induced emission of 4-amino-1,8-naphthalimide derivatives. To confirm this statement, 4-allylamino-1,8-naphthalimide 10 without a PET receptor was involved in the present study. The results obtained clearly showed that that lacks aggregation-induced emission in 4-amino-1,8-naphthalimides (Figure 13B); therefore, they are not suitable for solid state chemosensing probes.

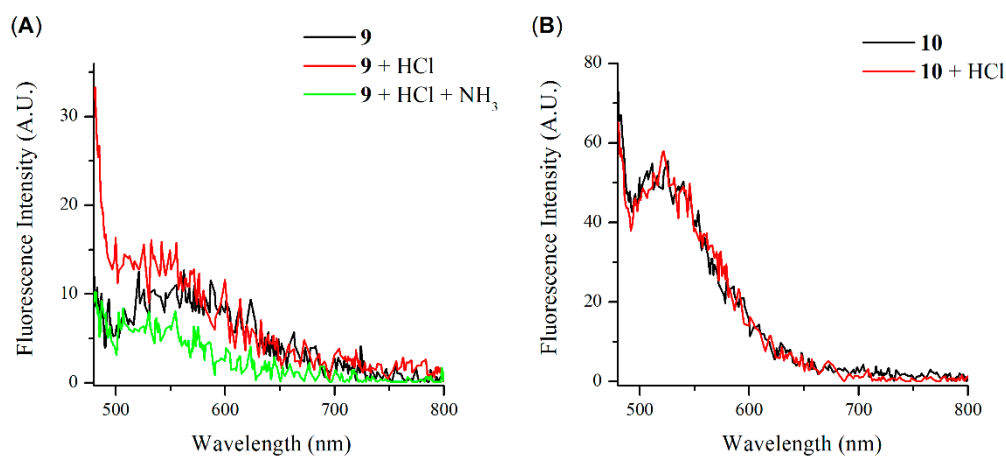


Figure 13. Fluorescence spectra of solid film ($\lambda_{\text{ex}} = 430 \text{ nm}$) of probe 9 (A), exposed first to HCl and then to NH_3 vapors, and compound 10 (B) exposed to HCl.

Furthermore, we found that, similarly to probe 9, compound 11 did not show any chemosensing fluorescence response toward HCl and NH_3 vapors in thin film (Figure 14), but the observed fluorescence output was on the opposite side compared to that of 9.

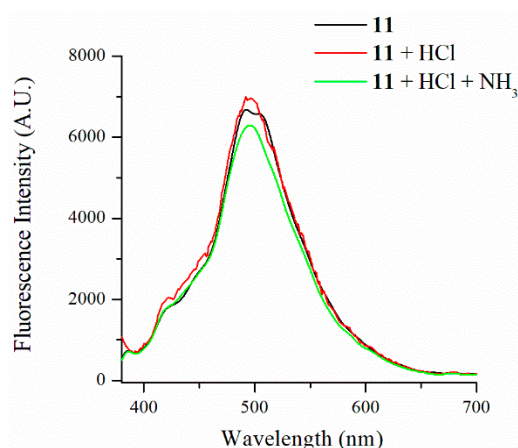


Figure 14. Fluorescence spectra of solid film of probe **11**, exposed first to HCl and then to NH₃ vapors ($\lambda_{\text{ex}} = 370$ nm).

In solid state, **11** showed a constant bright emission before and after exposure to HCl and NH₃ vapors in both thin film and strip papers. This effect can be easily explained by the presence of an acidic amide group and a basic methyl piperazine amine in **11**, whose intermolecular interaction favors and stabilizes the process of aggregate formation and AIE under the blocked PET process due to the engaged amine receptor. As a result, compound **11** showed well-pronounced AIE, but it was not suitable for a solid state emissive chemosensing probe due to the lacked PET quenching process.

All the results presented above clearly show the great potential of unsubstituted, 4-halogeno-substituted and 4-oxy-substituted 1,8-naphthalimides based on the classic PET “fluorophore-spacer-receptor” format to serve as chemosensing materials for acid/base vapors in aggregated state due to the simultaneous action of AIE and PET. The results presented here could be seen as a contribution to the development of the applied sensory chemistry from liquid solution toward solid support. The previous reports in this field were directed to synthesis of PET sensor beads, which required a complicated synthetic process for immobilization and utilization on polymer beads [38,70]. In contrast to the previous reports, the concept presented here was achieved simply and easily, especially since the covalent attachment to the surface of the polymer beads could not generate fluorescent aggregates; therefore, the resulting sensors showed only monomeric fluorescence emission as output. In particular, Thapa et al. prepared a dry-phase PET fluorescence sensor on a glass support; however, the sensing signal obtained after evaporation of a diluted solution of the fluorescent probe in its “off” or “on” state was a well-pronounced monomer emission [71], while the films in this study were obtained from concentrated solutions and showed the typical reaction for the 1,8-naphthalimides AIE. Similarly, the obtained strip papers also operated via AIE due to their preparation from high concentrated solutions of the PET probes (10^{-2} M) instead of the usually used diluted solutions (10^{-4} M), which resulted in a probe’s monomeric fluorescence [72].

4. Conclusions

In summary, we presented here the synthesis of a series of 1,8-naphthalimide derivatives and investigation of their ability to act as fluorescence-sensing materials for acid/base vapors in solid state via simultaneous photoinduced electron transfer (PET) and aggregation-induced emission (AIE). All compounds under study were designed as PET fluorescent probes based on a classical “fluorophore-spacer-receptor” model, where the electron-rich tertiary amine is the proton receptor and the 1,8-naphthalimide fluorophore is the fluorescence signaling part. The implemented investigation and the results obtained showed that the thin films and strip papers of 1,8-naphthalimide derivatives with “Upper-receptor”, which are unsubstituted in the C-4 position or the substituent, have a weak electron-donor or even electron-acceptor character, due to the fact that the generation of a weak repulsion

field in the fluorophore molecule could be used as an efficient platform for rapid detection of acid/base vapors in solid state. The study showed that the emission of the thin films was transferred between the “off” and “on” states reversibly at least 10 times without significant changes in both states and with considerable fluorescence enhancement. In addition, the ability of this type of 1,8-naphthalimides to determine pH in aqueous solution was studied, whereby it was found that the obtained strip papers are suitable indicators for determination of pHs in a pH window of 1.5–2.5. In contrast to “Upper-receptor” compounds, those with “Lower-receptor”, such as 4-amino and 4-amido 1,8-naphthalimides, turned out to be insufficiently suitable indicators for acid/base vapors in solid state.

Author Contributions: Conceptualization, V.B.B. and N.I.G.; methodology, N.I.G.; formal analysis, N.I.G. and V.V.B.; investigation, V.V.B. (synthesis and photochemistry); writing—original draft preparation, N.I.G.; writing—review and editing, V.B.B.; supervision, V.B.B.; funding acquisition, V.B.B. All authors have read and agreed to the published version of the manuscript.

Funding: This research was funded by National Science Fund of Bulgaria, grant number KP-06-H39/3.

Institutional Review Board Statement: Not applicable.

Informed Consent Statement: Not applicable.

Data Availability Statement: The authors declare that the data supporting the findings of this study are available within the article.

Conflicts of Interest: The authors declare no conflict of interest.

References

1. Steinegger, A.; Wolfbeis, O.S.; Borisov, S.M. Optical Sensing and Imaging of pH Values: Spectroscopies, Materials, and Applications. *Chem. Rev.* **2020**, *120*, 12357–12489. [[CrossRef](#)] [[PubMed](#)]
2. Mishra, S.; Singh, A.K. Optical sensors for water and humidity and their further applications. *Coord. Chem. Rev.* **2021**, *445*, 214063. [[CrossRef](#)]
3. Aderinto, S.; Imhanria, S. Fluorescent and colourimetric 1,8-naphthalimide-appended chemosensors for the tracking of metal ions: Selected examples from the year 2010 to 2017. *Chem. Pap.* **2018**, *72*, 1823–1851. [[CrossRef](#)]
4. Hamilton, G.; Sahoo, S.; Kamila, S.; Singh, N.; Kaur, N.; Hyland, B.; Callan, J. Optical probes for the detection of protons, and alkali and alkaline earth metal cations. *Chem. Soc. Rev.* **2015**, *44*, 4415–4432. [[CrossRef](#)] [[PubMed](#)]
5. Dian, J.; Jindřich, J.; Jelínek, I. Functionalized materials with fluorescent dyes for chemosensor applications. *Monatsh. Chem.* **2017**, *148*, 1929–1935. [[CrossRef](#)]
6. Huang, J.; Chen, Y.; Qi, J.; Zhou, X.; Niu, L.; Yana, Z.; Wang, J.; Zhao, G. A dual-selective fluorescent probe for discriminating glutathione and homocysteine simultaneously. *Spectrochim. Acta Part A* **2018**, *201*, 105–111. [[CrossRef](#)]
7. Georgiev, N.; Bryaskova, R.; Tzoneva, R.; Ugrinova, I.; Detrembleur, C.; Miloshev, S.; Asiri, A.; Qusti, A.; Bojinov, V. A novel pH sensitive water soluble fluorescent nanomicellar sensor for potential biomedical applications. *Bioorg. Med. Chem.* **2013**, *21*, 6292–6302. [[CrossRef](#)]
8. Yang, X.; Lovell, J.F.; Murthy, N.; Zhang, Y. Organic Fluorescent Probes for Diagnostics and Bio-Imaging. *Top. Med. Chem.* **2020**, *34*, 33–53.
9. Shen, R.; Qian, Y. A mitochondria-oriented fluorescent probe for ultrafast and ratiometric detection of HSO₃-Based on naphthalimide-hemicyanine. *New J. Chem.* **2019**, *43*, 7606–7612. [[CrossRef](#)]
10. Ismail, S.; Bryaskova, R.; Georgiev, N.; Philipova, N.; Uzunova, V.; Bakov, V.; Tzoneva, R.; Bojinov, V. Design and synthesis of fluorescent shell functionalized polymer micelles for biomedical application. *Polym. Adv. Technol.* **2020**, *31*, 1365–1376. [[CrossRef](#)]
11. Guo, F.-F.; Wu, W.-N.; Zhao, X.-L.; Wang, Y.; Fan, Y.-C.; Zhang, C.-X.; Xu, Z.-H. A deep-red lysosome-targetable fluorescent probe for detection of hypochlorous acid in pure water and its imaging application in living cells and zebrafish. *Spectrochim. Acta Part A* **2022**, *264*, 120270. [[CrossRef](#)]
12. Georgiev, N.; Said, A.; Toshkova, R.; Tzoneva, R.; Bojinov, V. A novel water-soluble perylenetetracarboxylic diimide as a fluorescent pH probe: Chemosensing, biocompatibility and cell imaging. *Dyes Pigment.* **2019**, *160*, 28–36. [[CrossRef](#)]
13. Hayashi, Y.; Suzuki, N.; Maeda, T.; Fujiwara, H.; Yagi, S. Photophysical properties of 4-(5-methylthiophen-2-yl)pyridinium-cyclic enolate betaine dyes tuned by control of twisted intramolecular transfer. *New J. Chem.* **2021**, *45*, 9770–9779. [[CrossRef](#)]
14. Zhang, H.; Xu, Z.; Tao, F.; Yu, W.W.; Cui, Y. Enhanced photostability of aggregation induced emission by hydrophobic groups. *Anal. Chim. Acta* **2021**, *1186*, 339076. [[CrossRef](#)]
15. Said, A.; Georgiev, N.; Bojinov, V. A novel dual naked eye colorimetric and fluorescent pH chemosensor and its ability to execute three INHIBIT based digital comparator. *Dyes Pigment.* **2022**, *205*, 110489. [[CrossRef](#)]

16. Zheng, P.; Abdurahman, A.; Zhang, Z.; Feng, Y.; Zhang, Y.; Ai, X.; Li, F.; Zhang, M. A simple organic multi-analyte fluorescent probe: One molecule realizes the detection to DNT, TATP and Sarin substitute gas. *J. Hazard. Mater.* **2021**, *409*, 124500. [[CrossRef](#)]
17. Krasteva, P.; Dimitrova, M.; Georgiev, N.; Bojinov, V. A novel 1,8-naphthalimide probe for selective determination of Hg²⁺ in a wide pH window. *J. Chem. Technol. Metall.* **2018**, *53*, 150–158.
18. Singh, H.; Bhargav, G.; Kumar, S.; Singh, P. Quadruple-signaling (PET, ICT, ESIPT, -C=N- rotation) mechanism-based dual chemosensor for detection of Cu²⁺ and Zn²⁺ ions: TRANSFER, INH and complimentary OR/NOR logic circuits. *J. Photochem. Photobiol. A Chem.* **2018**, *357*, 175–184. [[CrossRef](#)]
19. Anand, T.; Kumar, S.K.A.; Sahoo, S.K. A new Al³⁺ selective fluorescent turn-on sensor based on hydrazide-naphthalic anhydride conjugate and its application in live cells imaging. *Spectrochim. Acta Part A* **2018**, *204*, 105–112. [[CrossRef](#)]
20. Georgiev, N.; Asiri, A.; Qusti, A.; Alamry, K.; Bojinov, V. A pH sensitive and selective ratiometric PAMAM wavelength-shifting bichromophoric system based on PET, FRET and ICT. *Dyes Pigment.* **2014**, *102*, 35–45. [[CrossRef](#)]
21. Li, S.; Zhao, B.; Kan, W.; Wang, L.; Song, B.; Chen, S. A off-on pH fluorescence probe derived from phenanthro[9,10-d]imidazol-fluorescein based on ESIPT and ICT. *Res. Chem. Intermed.* **2018**, *44*, 491–502. [[CrossRef](#)]
22. Said, A.; Georgiev, N.; Bojinov, V. Low molecular weight probe for selective sensing of pH and Cu²⁺ working as three INHIBIT based digital comparator. *J. Fluoresc.* **2022**, *32*, 405–417. [[CrossRef](#)] [[PubMed](#)]
23. García, A.L.; Ochoa- Terán, A.; Tirado- Guízar, A.; Jara- Cortés, J.; Pina-Luis, G.; Santacruz Ortega, H.; Labastida- Galván, V.; Ordoñez, M.; Peón, J. Experimental and theoretical study of novel aminobenzamide-aminonaphthalimide fluorescent dyads with a FRET mechanism. *RSC Adv.* **2022**, *12*, 6192–6204. [[CrossRef](#)] [[PubMed](#)]
24. Alamry, K.; Georgiev, N.; Abdullah El-Daly, S.; Taib, L.; Bojinov, V. A ratiometric rhodamine-naphthalimide pH selective probe built on the basis of a PAMAM light-harvesting architecture. *J. Lumin.* **2015**, *158*, 50–59. [[CrossRef](#)]
25. Ozdemir, M. Two colorimetric and fluorescent dual-channel chemosensors for the selective detection of pH in aqueous solutions. *ChemistrySelect* **2020**, *5*, 14340–14348. [[CrossRef](#)]
26. Georgiev, N.; Dimitrova, M.; Todorova, Y.; Bojinov, V. Synthesis, chemosensing properties and logic behaviour of a novel ratiometric 1,8-naphthalimide probe based on ICT and PET. *Dyes Pigment.* **2016**, *131*, 9–17. [[CrossRef](#)]
27. Bakov, V.V.; Georgiev, N.I.; Bojinov, V.B. A novel fluorescent probe for determination of pH and viscosity based on a highly water-soluble 1,8-naphthalimide rotor. *Molecules* **2022**, *27*, 7556. [[CrossRef](#)]
28. Seraj, S.; Rouhani, S.; Faridbod, F. Naphthalimide-based optical turn-on sensor for monosaccharide recognition using boronic acid receptor. *RSC Adv.* **2019**, *9*, 17933–17940. [[CrossRef](#)]
29. Marinova, N.; Georgiev, N.; Bojinov, V. Design, synthesis and pH sensing properties of novel 1,8-naphthalimide-based bichromophoric system. *J. Photochem. Photobiol. A Chem.* **2011**, *222*, 132–140. [[CrossRef](#)]
30. Yao, C.; Lin, H.; Crory, H.; de Silva, A.P. Supra-molecular agents running tasks intelligently (SMARTI): Recent developments in molecular logic-based computation. *Mol. Syst. Des. Eng.* **2020**, *5*, 1325–1353. [[CrossRef](#)]
31. Georgiev, N.; Krasteva, P.; Bakov, V.; Bojinov, V. A highly water-soluble and solid state emissive 1,8-naphthalimide as a fluorescent PET probe for determination of pHs, acid/base vapors, and water content in organic solvents. *Molecules* **2022**, *27*, 4229. [[CrossRef](#)]
32. Panchenko, P.A.; Fedorov, Y.V.; Fedorova, O.A. Selective fluorometric sensing of Hg²⁺ in aqueous solution by the inhibition of PET from dithia-15-crown-5 ether receptor conjugated to 4-amino-1,8-naphthalimide fluorophore. *J. Photochem. Photobiol. A Chem.* **2018**, *364*, 124–129. [[CrossRef](#)]
33. Georgiev, N.I.; Sakr, A.R.; Bojinov, V.B. Design and synthesis of a novel PET and ICT based 1,8-naphthalimide FRET bichromophore as a four-input Disabled-Enabled-OR logic gate. *Sens. Actuators B Chem.* **2015**, *221*, 625–634. [[CrossRef](#)]
34. Spiteri, J.C.; Johnson, A.D.; Denisov, S.A.; Jonusauskas, G.; McClenaghan, N.D.; Magri, D.C. A fluorescent AND logic gate based on a ferrocene-naphthalimide-piperazine format responsive to acidity and oxidizability. *Dyes Pigment.* **2018**, *157*, 278–283. [[CrossRef](#)]
35. Wright, G.D.; Yao, C.; Moody, T.S.; de Silva, A.P. Fluorescent molecular logic gates based on photoinduced electron transfer (PET) driven by a combination of atomic and biomolecular inputs. *Chem. Commun.* **2020**, *56*, 6838–6841. [[CrossRef](#)]
36. Said, A.; Georgiev, N.; Bojinov, V. A smart chemosensor: Discriminative multidetection and various logic operations in aqueous solution at biological pH. *Spectrochim. Acta Part A* **2019**, *223*, 117304. [[CrossRef](#)]
37. Chi, W.; Chen, J.; Qiao, Q.; Gao, Y.; Xu, Z.; Liu, X. Revealing the switching mechanisms of an OFF-ON-OFF fluorescent logic gate system. *Phys. Chem. Chem. Phys.* **2019**, *21*, 16798–16803. [[CrossRef](#)]
38. Refalo, M.V.; Spiteri, J.C.; Magri, D.C. Covalent attachment of a fluorescent 'Pourbaix sensor' onto a polymer bead for sensing in water. *New J. Chem.* **2018**, *42*, 16474–16477. [[CrossRef](#)]
39. de Silva, A.P. Crossing the divide: Experiences of taking fluorescent PET (photoinduced electron transfer) sensing/switching systems from solution to solid. *Dyes Pigment.* **2022**, *204*, 110453. [[CrossRef](#)]
40. Georgiev, N.I.; Bryaskova, R.G.; Ismail, S.R.; Philipova, N.D.; Uzunova, V.P.; Bakov, V.V.; Tzoneva, R.D.; Bojinov, V.B. Aggregation induced emission in 1,8-naphthalimide embedded nanomicellar architecture as a platform for fluorescent ratiometric pH-probe with biomedical applications. *J. Photochem. Photobiol. A Chem.* **2021**, *418*, 113380. [[CrossRef](#)]
41. Huang, P.-Y.; Gao, J.-Y.; Song, C.-Y.; Hong, J.-L. Ionic complex of a rhodamine dye with aggregation-induced emission properties. *Faraday Discuss.* **2017**, *196*, 177–190. [[CrossRef](#)] [[PubMed](#)]
42. Mei, J.; Leung, N.; Kwok, R.; Lam, J.; Tang, B. Aggregation-induced emission: Together we shine, united we soar! *Chem. Rev.* **2015**, *115*, 11718–11940. [[CrossRef](#)] [[PubMed](#)]

43. Kwok, R.; Leung, C.; Lam, J.; Tang, B. Biosensing by luminogens with aggregation-induced emission characteristics. *Chem. Soc. Rev.* **2015**, *44*, 4228–4238. [[CrossRef](#)] [[PubMed](#)]
44. Mukherjee, S.; Thilagar, P. Fine-tuning solid-state luminescence in NPIs (1,8-naphthalimides): Impact of the molecular environment and cumulative interactions. *Phys. Chem. Chem. Phys.* **2014**, *16*, 20866–20877. [[CrossRef](#)] [[PubMed](#)]
45. Shi, X.; Yan, N.; Niu, G.; Sung, S.; Liu, Z.; Liu, J.; Kwok, R.K.; Lam, J.; Wang, W.; Sung, H.; et al. In vivo monitoring of tissue regeneration using a ratiometric lysosomal AIE probe. *Chem. Sci.* **2020**, *11*, 3152–3163. [[CrossRef](#)]
46. Georgiev, N.I.; Bakov, V.V.; Bojinov, V.B. A solid-state-emissive 1,8-naphthalimide probe based on photoinduced electron transfer and aggregation-induced emission. *ChemistrySelect* **2019**, *4*, 4163–4167. [[CrossRef](#)]
47. Georgiev, N.I.; Dimov, S.; Asiri, A.; Alamry, K.; Obaid, A.; Bojinov, V.B. Synthesis, selective pH-sensing activity and logic behavior of highly water-soluble 1,8-naphthalimide and dihydroimidazonaphthalimide derivatives. *J. Lumin.* **2014**, *149*, 325–332. [[CrossRef](#)]
48. Dimov, S.M.; Georgiev, N.I.; Asiri, A.M.; Bojinov, V.B. Synthesis and Sensor Activity of a PET-based 1,8-naphthalimide Probe for Zn²⁺ and pH Determination. *J. Fluoresc.* **2014**, *24*, 1621–1628. [[CrossRef](#)]
49. Ramachandram, B.; Sankaran, N.; Karmakar, R.; Saha, S.; Samanta, A. Fluorescence signalling of transition metal ions by multi-component systems comprising 4-chloro-1,8-naphthalimide as fluorophore. *Tetrahedron* **2000**, *56*, 7041–7044. [[CrossRef](#)]
50. Ramachandram, B.; Saroja, G.; Sankaran, N.; Samanta, A. Unusually high fluorescence enhancement of some 1,8-naphthalimide derivatives induced by transition metal salts. *J. Phys. Chem. B* **2000**, *104*, 11824–11832. [[CrossRef](#)]
51. Bojinov, V.; Grabchev, I. A new method for synthesis of 4-allyloxy-1,8-naphthalimide derivatives for use as fluorescent brighteners. *Dyes Pigment.* **2001**, *51*, 57–61. [[CrossRef](#)]
52. Chen, J.; Tang, R.; Luo, Z.; Yang, C. Solvatofluorochromism of *N*-[2-(2-hydroxyethylamino)-ethyl]-1,8-naphthalimide in protic solvent. *J. Mol. Struct.* **2009**, *917*, 170–175. [[CrossRef](#)]
53. Saini, A.; Bhasin, A.; Singh, N.; Kaur, N. Development of a Cr(III) ion selective fluorescence probe using organic nanoparticles and its real time applicability. *New J. Chem.* **2016**, *40*, 278–284. [[CrossRef](#)]
54. Jin, R.; Ahmad, I. Theoretical study on photophysical properties of multifunctional star-shaped molecules with 1,8-naphthalimide core for organic light-emitting diode and organic solar cell application. *Theor. Chem. Acc.* **2015**, *134*, 89. [[CrossRef](#)]
55. Gunnlaugsson, T.; McCoy, C.; Morrow, R.; Phelan, C.; Stomeo, F. Towards the development of controllable and reversible ‘on-off’ luminescence switching in soft-matter; synthesis and spectroscopic investigation of 1,8-naphthalimide-based PET (photoinduced electron transfer) chemosensors for pH in water-permeable hydrogels. *ARKIVOC* **2003**, *7*, 216–228. [[CrossRef](#)]
56. de Silva, A.P.; Gunaratne, H.; Habib-Jiwan, J.-L.; McCoy, C.; Rice, T.; Soumillion, J.-P. New fluorescent model compounds for the study of photoinduced electron transfer: The influence of molecular electric field in the excited state. *Angew. Chem. Int. Ed. Engl.* **1995**, *34*, 1728–1731. [[CrossRef](#)]
57. Wang, L.; Wang, G.; Shang, C.; Kang, R.; Fang, Y. Naphthalimide-based fluorophore for soft anionic interface monitoring. *ACS Appl. Mater. Interfaces* **2017**, *9*, 35419–35426. [[CrossRef](#)]
58. Georgiev, N.I.; Marinova, N.V.; Bojinov, V.B. Design and synthesis of light-harvesting rotor based on 1,8-naphthalimide units. *J. Photochem. Photobiol. A Chem.* **2020**, *401*, 112733. [[CrossRef](#)]
59. Liu, J.; de Silva, A.P. Path-selective photoinduced electron transfer (PET) in a membrane-associated system studied by pH-dependent fluorescence. *Inorg. Chim. Acta* **2012**, *381*, 243–246. [[CrossRef](#)]
60. Georgiev, N.I.; Bojinov, V.B.; Nikolov, P.S. The design, synthesis and photophysical properties of two novel 1,8-naphthalimide fluorescent pH sensors based on PET and ICT. *Dyes Pigment.* **2011**, *88*, 350–357. [[CrossRef](#)]
61. de Silva, A.P.; Rice, T. A small supramolecular system which emulates the unidirectional, path-selective photoinduced electron transfer (PET) of the bacterial photosynthetic reaction centre (PRC). *Chem. Commun.* **1999**, *2*, 163–164. [[CrossRef](#)]
62. Georgiev, N.I.; Dimitrova, M.D.; Mavrova, A.T.; Bojinov, V.B. Synthesis, fluorescence-sensing and molecular logic of two water-soluble 1,8-naphthalimides. *Spectrochim. Acta Part A* **2017**, *183*, 7–16. [[CrossRef](#)] [[PubMed](#)]
63. Georgiev, N.; Krasteva, P.; Bojinov, V. A ratiometric 4-amido-1,8-naphthalimide fluorescent probe based on excimer-monomer emission for determination of pH and water content in organic solvents. *J. Lumin.* **2019**, *212*, 271–278. [[CrossRef](#)]
64. Mati, S.; Chall, S.; Bhattacharya, S. Aggregation-induced fabrication of fluorescent organic nanorings: Selective biosensing of cysteine and application to molecular logic gate. *Langmuir* **2015**, *31*, 5025–5032. [[CrossRef](#)] [[PubMed](#)]
65. Soni, M.; Das, S.; Sahu, P.; Kar, U.; Rahaman, A.; Sarkar, M. Synthesis, photophysics, live cell imaging, and aggregation behavior of some structurally similar alkyl chain containing bromonaphthalimide systems: Influence of alkyl chain length on the aggregation behavior. *J. Phys. Chem. C* **2013**, *117*, 14338–14347. [[CrossRef](#)]
66. Li, X.; Chen, H.; Kirillov, A.; Xie, Y.; Shan, C.; Wang, B.; Shia, C.; Tang, Y. A paper-based lanthanide smart device for acid–base vapour detection, anti-counterfeiting and logic operations. *Inorg. Chem. Front.* **2016**, *3*, 1014–1020. [[CrossRef](#)]
67. Martinez, A.W.; Phillips, S.T.; Whitesides, G.M. Diagnostics for the developing world: Microfluidic paper-based analytical devices. *Anal. Chem.* **2010**, *82*, 3–10. [[CrossRef](#)]
68. Nery, E.W.; Kubota, L.T. Sensing approaches on paper-based devices: A review. *Anal. Bioanal. Chem.* **2013**, *405*, 7573–7595. [[CrossRef](#)]
69. Cate, D.M.; Adkins, J.A.; Mettakoonpitak, J.; Henry, C.S. Recent developments in paper-based microfluidic devices. *Anal. Chem.* **2015**, *87*, 19–41. [[CrossRef](#)]

70. Nath, S.; Maitra, U. A simple and general strategy for the design of fluorescent cation sensor beads. *Org. Lett.* **2006**, *8*, 3239–3242. [[CrossRef](#)]
71. Thapa, P.; Arnquist, I.; Byrnes, N.; Denisenko, A.A.; Foss, F.W., Jr.; Jones, B.J.P.; McDonald, A.D.; Nygren, D.R.; Woodruff, K. Barium chemosensors with dry-phase fluorescence for neutrinoless double beta decay. *Sci. Rep.* **2019**, *9*, 15097. [[CrossRef](#)]
72. Ling, J.; Naren, G.; Kelly, J.; Moody, T.S.; de Silva, A.P. Building pH sensors into paper-based small-molecular logic systems for very simple detection of edges of objects. *J. Am. Chem. Soc.* **2015**, *137*, 3763–3766. [[CrossRef](#)]